

The ESO-Sculptor Survey: Galaxy Populations and Luminosity Function at $z \leq 0.5$

Gaspar Galaz¹ and Valérie de Lapparent²

¹*Observatories of the Carnegie Institution of Washington. Las Campanas Observatory. Casilla 601, La Serena, Chile (gaspar@ociw.edu)*

²*Institut d'Astrophysique de Paris, CNRS. 98bis, Boulevard Arago, 75014, Paris, France (lapparen@iap.fr)*

Abstract. We briefly show results on the redshift and space distribution of field galaxies with different spectral types in the ESO-Sculptor survey (ESS). We also show results on the ESS galaxy luminosity function.

1 Introduction: The ESO-Sculptor Survey

The ESO-Sculptor Survey [11] provides photometric and spectroscopic data of galaxies from a narrow, but deep, patch of the sky. Data were gathered at La Silla Observatory (ESO), using both the 3.6m telescope and the NTT. The photometric catalogue covers a continuous strip of 1.53° (R.A.) \times 0.24° (DEC.) \sim 0.37 deg^2 in the Sculptor constellation, with center (J2000) \sim $0^h 21^m, -30^\circ$, and 17° from the south galactic pole. A detailed description of the construction and reduction of the photometric catalogue can be found in [1].

The spectroscopic catalogue contains the spectra and redshifts of \sim 700 galaxies with $R = 20.5$, obtained using multi-slit spectroscopy. Details on the reduction of the spectroscopic data are in [3]. The ESS has already provided some results on our view of the distribution of galaxies at large-scale to $z \sim 0.5$ [4]. Here we describe recent results on the proportion and distribution of the different types of galaxies, provided by a spectral classification approach based on the principal component analysis (PCA) [14]. This spectral classification is fundamental to have insights on the distribution of different galaxy types which populate the large-scale structures up to $z \sim 0.5$. Furthermore, it allows to compute K-corrections which in turn allow to have rest-frame magnitudes to construct the galaxy luminosity function (LF). These main results follow.

2 Galaxy Populations

Understanding the formation and evolution of galaxies [2] requires a detailed knowledge of the different galaxy populations as a function of redshift and in terms of the local density. In order to obtain an unbiased description of the different galaxy populations for the ESS, we have used a spectral classification approach which is more tightly related to the underlying physics and to the

stellar populations which characterize the galaxies, than would be a morphological classification. Morphological classifications also have the inconvenient of being filter and redshift dependent. The PCA spectral classification for the ESS was made using only spectra taken during spectro-photometric nights, because PCA galaxy spectral types are partly determined by the shape of the continuum [5]. A sub-sample of 330 spectra were analyzed in the spectral range $\lambda = 3700 - 5250 \text{ \AA}$, where the best compromise in terms of spectral coverage and number of spectra is obtained. The PCA allows to generate a *spectral classification plane* for galaxies, which provides a continuous spectral sequence for the ESS (labeled from I [early types] to VI [late types]). All details on the ESS spectral classification are provided in [9].

The analysis of the ESS spectral types as a function of redshift, shows that there is *no* significant evolution of different spectral types up to $z \sim 0.5$. Except for an excess of early-type galaxies at $z \sim 0.43$ (caused by a large galaxy concentration), the distribution per redshift is nearly uniform for each spectral type as a function of redshift (see Figure 1). Another important result is related to the morphology-density relationship [6]. The distribution of different spectral types as a function of the local density shows that most of the early-type galaxies ($\sim 85\%$) are associated to galaxy groups. Late-type galaxies, on the other hand, occupy nearly uniformly both the low and high density regions.

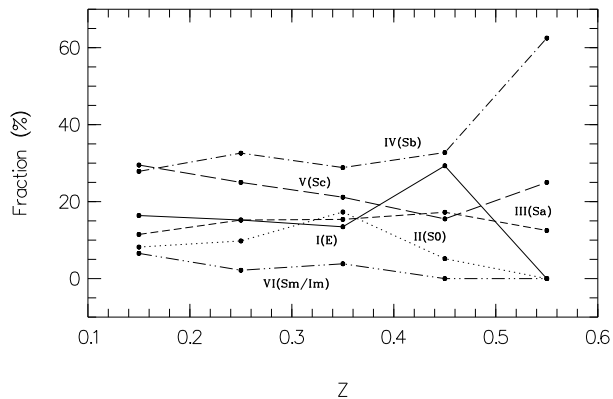


Figure 1: The redshift distribution of the different PCA spectral types in the ESS. Spectral types are labeled in roman. Few galaxies are detected at $z > 0.5$. See text for details.

3 The ESS Luminosity Function

The projection of spectrophotometric templates onto the ESS classification plane [9] allows to compute K-corrections based on the spectral classification. This analysis requires the use of synthetic spectra which allow to “extrapolate” the ESS spectra in the standard filters when these are not included in the spectral range of the observed spectra. We have used the PEGASE models [8] using a star formation rate proportional to the amount of gas, and solar metallicity. Ages range from 0.1 Gyr to 16 Gyr. For each ESS spectrum, the closest projected model onto the classification plane (with the same wavelength interval as for the ESS spectrum) is taken as its most similar model spectrum. Synthetic photometry is done onto the model spectra using the B_j , V_j and R_c ESS passbands and K-corrections are computed following their definition [15]. Although this approach depends on the model which is used, the source of difference from one model to another can be controlled. These K-corrections are more reliable than those obtained by the standard approach of using morphological classification and making strong hypotheses on the relationship between the spectral energy distributions (SEDs) and the morphological types. Measuring the K-corrections is one of the fundamental steps to construct the galaxy luminosity function (LF).

The ESS LF was calculated using standard maximum likelihood techniques, including a non-parameterized (EEP method, [7]) and a parameterized functional form (using the STY method, [16]). For the latter, we adopt the Schechter function. Maximum likelihood methods ensure that the LF is not biased by the large-scale inhomogeneities present in the catalogue. The best-fit Schechter function for the ESS LF in R_c ($M^* = -21.15 \pm 0.19 + 5 \log h$, $\alpha = -1.23 \pm 0.13$ and $\phi^* = 0.0203 \pm 0.008h^3 \text{ Mpc}^{-3}$ ($q_0 = 0.5$, $H_0 = 100 \text{ km s}^{-1} \text{ Mpc}^{-1}$) is shown as a bold line in Figure 2. Symbols represent the EEP non parameterized LF. The 1-sigma error ellipse for the Schechter parameters is shown in the inset. The R_c band LF was constructed from 327 ESS galaxies with PCA spectral types, and corrected for incompleteness effects following the method described in [17]. Figure 2 also shows the LF of other surveys, transformed into the R_c band. The LF for the ESS is in good agreement with the LF for the CNOC1 survey ([13], long-dashed line), the ESO-Slice project (hereafter ESP, [18]; dotted line), and the Century survey ([10], short-dashed line). The LF for the LCRS ([12], dash-dotted line) is different from the other LFs, in particular at the faint end. Selection effects in that survey are probably responsible for the loss of a large number of (faint) blue galaxies [12]. Like in other surveys (in particular the ESP and the CNOC1 survey), we note that the faint end of the LF follows an exponential form for magnitudes fainter than $M_{Rc} = -18$. Most of the galaxies which occupy this magnitude range are galaxies with spectral types later than IV (see Figure 1). 82% of these galaxies show evidence for present star formation, as measured by the $[\text{OII}]3727\text{\AA}$ emission line. More than 80% of the galaxies which have $M_{Rc} < M^*$ have spectral types earlier than III, and very few (<2%) show evidence for star formation.

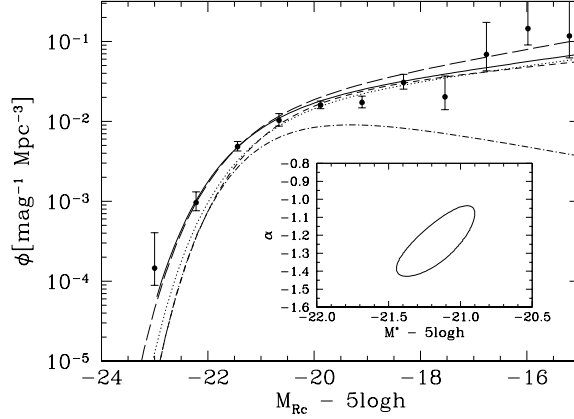


Figure 2: The ESS galaxy luminosity function (LF) in the R_c (Cousins) filter. The bold line represents the best-fit Schechter LF function (see text for details). LFs for other surveys are also shown using their Schechter fit: the ESP, dotted line [18]; the CNOC1, long-dashed [13]; the Century Survey, short-dashed [10]; the LCRS, dot-dashed [12]. The inset shows the 1-sigma error ellipse for the ESS Schechter LF. Points with error bars represent the ESS non-parameterized (EEP) LF.

Acknowledgements. GG acknowledge Institut d’Astrophysique de Paris and Carnegie Observatories support for this work.

References

- [1] Arnouts, S. et al. 1997, A&AS 124, 163
- [2] Baugh, C., Cole, S. & Frenk, C. 1996, MNRAS 283, 1361
- [3] Bellanger, C. et al. 1995, A&AS 110, 159
- [4] Bellanger, C. & de Lapparent, V. 1995, ApJ 455, L103
- [5] Connolly, A. et al. 1995, AJ 110, 1071
- [6] Dressler, A. et al. 1997, ApJ 490, 577
- [7] Efsthathiou, G., Ellis, R. & Peterson, B. 1988, MNRAS 232, 431 (EEP)
- [8] Fioc, M. & Rocca-Volmerange, B. 1997, A&A 326, 950
- [9] Galaz, G. & de Lapparent, V. 1998, A&A 332, 459
- [10] Geller, M. et al. 1997, AJ 114, 2205
- [11] de Lapparent et al. 1997, The Messenger, 89, 21
- [12] Lin, H. et al. 1996, ApJ 464, 60
- [13] Lin, H., Yee, H., Carlberg, R., Ellingson, E. 1997, ApJ 475, 494
- [14] Murtagh, F. & Heck, A. 1987, *Multivariate Data Analysis*, Reidel
- [15] Oke, J. & Sandage, A. 1968, ApJ 154, 210
- [16] Sandage, A., Tammann, G. & Yahil, A. 1979, ApJ 232, 352 (STY)
- [17] Zucca, E., Pozzetti, L. & Zamorani, G. 1994, MNRAS 269, 953
- [18] Zucca, E. et al. 1997, A&A 326, 477